Mon. Not. R. Astron. Soc. **000**, 1–10 (2011) Printed 30 March 2015 (MN LATEX style file v2.2)

Small-N collisional dynamics II: Roaming the realm of not-so-small-N

Nathan W. C. Leigh[1,2], Aaron M. Geller[3,4] ⋆

[1] *Department of Astrophysics, American Museum of Natural History, Central Park West and 79th Street, New York, NY 10024*
[2] *Department of Physics, University of Alberta, CCIS 4-183, Edmonton, AB T6G 2E1, Canada*
[3] *Center for Interdisciplinary Exploration and Research in Astrophysics (CIERA) and Department of Physics and Astronomy, Northwestern University, 2145 Sheridan Rd, Evanston, IL 60208, USA*
[4] *Department of Astronomy and Astrophysics, University of Chicago, 5640 S. Ellis Avenue, Chicago, IL 60637*

30 March 2015

ABSTRACT

We develop a formalism for calculating probabilities for the outcomes of stellar dynamical interactions, based on results from N-body scattering experiments. We focus here on encounters involving up to six particles and calculate probabilities for direct stellar collisions; however our method is in principle valid for larger particle numbers. Our method relies on the binomial theorem, and is applicable to encounters involving any combination of particle radii. We further demonstrate that our base model is valid to within a few percent for any combination of particle masses, provided the minimum mass ratio is within a factor of a few from unity. This method is particularly suitable for models of collisional systems involving large numbers of stars, such as globular clusters, old open clusters and galactic nuclei, where small subsets of stars may regularly have very close encounters, and the direct integration of all such encounters is computationally expensive. Variations of our method may also be used to treat other encounter outcomes, such as ejections and exchanges.

Key words: gravitation – binaries (including multiple): close – globular clusters: general – stars: kinematics and dynamics – scattering – methods: analytical.

1 INTRODUCTION

The three-body problem has a long history extending all the way back to Newton (1686), yet it has never been fully solved analytically. Indeed, for the majority of the relevant parameter space and over sufficiently long timescales, the evolution is chaotic (Poincare 1892). More recently, a number of different approaches have been invoked to study the problem (e.g. Henon 1969; Valtonen & Karttunen 2006), and the most common approach today is to use computers to integrate the equations of motion directly (in some instances, using the secular approximation, e.g. Naoz & Fabrycky 2014). And yet, in modern N-body simulations of star cluster evolution, it is the presence of binaries and especially higher-order multiples that poses the biggest computational challenge. The time evolution of the orbits within multiple star systems, as well as the outcomes of chaotic close gravitational encounters involving multiples, requires very small time steps, relative to the crossing time of the entire cluster (e.g. Hurley et al. 2005; Geller, Hurley & Mathieu 2013). This is particularly problematic, since simulations have shown that encounters involving binaries and triples can be crucial to not only the overall cluster evolution (e.g. Hut 1983a; Hut, McMillan & Romani 1992), but also the formation of exotic populations such as blue stragglers (Perets & Fabrycky 2009; Leigh & Sills 2011; Geller, Hurley & Mathieu 2013; Naoz & Fabrycky 2014) and even black holes (Mapelli & Zampieri 2014). What's more, observations have now revealed that higher-order multiple star systems are present in young star clusters in non-negligible numbers (e.g. Leigh et al. 2013).

One avenue into alleviating the computational challenges of directly integrating these relatively low-N systems (where N is the number of particles involved in the interaction) is to assume that the final states specifying the outcomes of chaotic gravitational interactions are probabilistic, as opposed to deterministic, in so far as how they relate to the initial encounter conditions. For example, a strongly interacting three-body system typically breaks up to produce a binary and an escaping star. Monaghan (1976a) showed that, by making the assumption that the probability of a configuration is proportional to the associated volume in phase-space, the statistical properties of the remaining bi-

⋆ E-mail: nleigh@ualberta.ca (NWCL), a-geller@northwestern.edu

nary and the escaper can be predicted (Monaghan 1976b). This result rests heavily on Liouville's Theorem (Liouville 1838), which states that, in a gravitionally-interacting system of particles, the total volume in phase-space is conserved in time.

In this, and our previous paper (Paper I; Leigh & Geller 2012), we develop a probabilistic interpretation of the outcomes of stellar encounters involving modest numbers of particles, with an over-arching goal of connecting the small- and large-N limits in bound configurations of finite-sized particles evolving under the influence of Newtonian gravity. In Paper I, we performed numerical scattering experiments involving single, binary and triple stars, using the `FEWBODY` code (Fregeau et al. 2004), and showed that the probability of a collision occuring during a chaotic gravitational interaction involving N identical particles is proportional to N^2. Interestingly, this same N-dependence is what is predicted by the mean-free path approximation in the limit of very large N.

In this paper, we delve further into the physical origin of this N-dependence, which relates to the binomial theorem, and explain how to exploit it to predict collision probabilities over a large range in the relevant parameter space of initial conditions with minimal computational expense. Specifically, here we simulate encounters involving *different types of particles* (whereas in Paper I we limited our study to identical particles). We focus first on encounters involving particles with identical masses but different physical radii, and outcomes that result in a single direct collision between any two particles. We then go on to consider encounters involving particles with different masses. In Section 2, we present our method for calculating probabilities for the encounter outcomes (focusing on collisions, but with a discussion of how to expand these results to different outcomes). Our results are presented in Section 3, which are then summarized and dicussed in Section 4.

2 METHOD

In this section, we present our method for calculating collision probabilities for encounters involving different types of particles, as well as the numerical scattering experiments used to test our extrapolation technique. We will focus first on encounters where the particle masses are all identical, but two different particle radii are possible. However, we keep our approach as general as possible, since in principle it can be extended to any combination of particle numbers and types. Later we relax the constraint of equal particle masses and begin a comparison to encounters involving particles of different masses.

2.1 Model

The key result from Paper I can be explained as follows. First, we showed that the probability of a collision occuring during a chaotic gravitational interaction involving N identical particles is proportional to N^2. (Note that a proportionality of $N(N-1)$ also fits the data; however we could not differentiate between these N-dependences at a statistically significant level.) We briefly touched upon a connection between this result and the large-N limit via the mean free path approximation. Specifically, in the limit of very large N, the mean free path approximation predicts that the rate of collisions between any two particles also scales as N^2. The physical origin of this proportionality can be traced back to the binomial theorem.[1]

Briefly, the binomial theorem states that the number of subsets composed of k particles that can be constructed from a larger sample composed of N particles is equal to:

$$\binom{N}{k} = \frac{N!}{(N-k)!k!} \tag{1}$$

Thus, in our specific example of collisions, we want the probability of selecting any two particles at random from our larger sample of N *identical* particles. From the binomial theorem, the number of ways to select any two particles is:

$$\binom{N}{2} = \frac{N!}{(N-2)!2!} = \frac{N(N-1)}{2} \tag{2}$$

This factor of $N(N-1)$ is proportional to the trend in collision probability as a function of N particles that we found in Paper I (as stated above). Furthermore, $N^2 \sim N(N-1)$ for $N \gg 1$, which is the scaling predicted by the mean free path approximation for collisions between any two particles. That is, the probability of any two identical particles colliding is proportional to Equation 2. In this way, the binomial theorem will form the backbone of any theory aiming to predict the relative probabilities of colliding two specific particles during a chaotic gravitational interaction.

What if the particles are not identical? Specifically, let us consider the case of *two* different particles, types 1 and 2. Three different collision scenarios are now possible; a collision between two particles of type 1, a collision between two particles of type 2 and a collision between a particle of type 1 and a particle of type 2. Thus, the collision probability can be broken up into the sum of three different terms, each corresponding to the probability of a specific collision event occurring:

$$P_{\rm coll} = P_{11} + P_{12} + P_{22}, \tag{3}$$

where P_{11} and P_{22} are the probabilities for a collision between two particles of type 1 and two particles of type 2, respectively, and P_{12} is the probability for a collision between a particle of type 1 and a particle of type 2. Now, the dependence of each of these probability terms depends on the number of particles of each type $N_{\rm i}$, and this $N_{\rm i}$-dependence comes from the binomial theorem.

Let N_1 and N_2 be the numbers of particles of type 1 and type 2, respectively, that are involved in the dynamical encounter. Then, Equation 3 can be re-written as:

$$P_{\rm coll} = \alpha_{11}\binom{N_1}{2} + \alpha_{12}\binom{N_1}{1}\binom{N_2}{1} + \alpha_{22}\binom{N_2}{2}, \tag{4}$$

where α_{11}, α_{12} and α_{22} are constants that depend on the

[1] More technically, the binomial theorem gives the different possible pairs of objects that could collide directly, and provides a good intuitive basis for building our model for the collision probability. Hence, our model implicitly assumes that other effects relevant to deciding the outcome of a chaotic gravitational encounter, and hence the collision probability, do not also depend on the number of interacting stars N.

total encounter energy E, the total angular momentum L and the properties of the particles (mass and radius).

We further assume that the particles have identical masses but two different radii are possible, namely R_1 and R_2 for particle types 1 and 2, respectively. We assume that the constant α_{12} can be found directly from the constants α_{11} and α_{22}:

$$\alpha_{12} = \frac{\alpha_{11}\sigma_{11} + \alpha_{22}\sigma_{22}}{\sigma_{11} + \sigma_{22}}, \quad (5)$$

where σ_{11} and σ_{22} are the collisional cross-sections for direct collisions between two particles of type 1 and two particles of type 2, respectively. The particles have identical masses, so the collisional cross-sections for these two collision scenarios are independent of mass and are set equal to the sum of their geometrical cross-sections, or $\sigma_{11} = 2\pi R_1^2$ (for example). Hence, from Equation 5, the constant α_{12} is calculated as the mean of the constants α_{11} and α_{22}, weighted by the corresponding geometrical cross-sections.

Equations 4 and 5 can be understood as follows. During the evolution of a chaotic gravitational encounter, stars are continually undergoing close approaches with each other. The probability of a close approach corresponding to a separation smaller than the sum of the particle radii occurring over the course of a crossing time is proportional to the number of interacting stars. That is, over a given period of time, more close approaches occur if more particles are involved (Valtonen & Karttunen 2006). However, if all particles are identical, then the probability of an event occurring (e.g. collision, ejection, etc.) in a crossing time is the same for all particles. Hence, identical particles have the same probability of experiencing a close approach corresponding to a separation smaller than the sum of the particle radii (which we call a collision). If the particles are *not* identical, then the volume of phase-space corresponding to a collision depends on the types of the colliding particles. The constants α_{11}, α_{12} and α_{22} in Equation 5 correct for these different phase-space volumes for different collision scenarios, which we assume are (non-linearly) proportional to their respective collisional cross-sections.

The key point is that, knowing a priori the constants α_{11} and α_{22} (i.e. from numerical scattering experiments), the collision probabilities for the remaining $N-1$ different interaction scenarios[2] can be calculated directly without the need for any additional numerical scattering experiments. As we will show in Section 3, for a given total encounter energy and angular momentum, a relatively small set of numerical scattering experiments can be extrapolated from to directly obtain the coefficients α_{11} and α_{22} for *any* particle radii. Additionally, numerical scattering experiments need only be run for the 2+2 or 1+3 cases[3] since, using the binomial theorem, the corresponding coefficients for higher-N interactions (2+3, 3+3, etc.) can be calculated directly. This offers a strategy for using a minimal number of numerical scattering experiments to calculate collision probabilities for encounters involving any number of particles with any combination of particle radii.

2.2 Numerical scattering experiments

In this section, we present the numerical scattering experiments used to test our strategy for calculating collision probabilities presented in the previous section.

We calculate the outcomes of a series of binary-binary, single-triple, binary-triple, and triple-triple encounters using the `FEWBODY` numerical scattering code[4]. The code integrates the usual N-body equations in configuration- (i.e., position-) space in order to advance the system forward in time. For details concerning the adaptive integration, classification techniques, etc. used by `FEWBODY`, we refer the reader to Fregeau et al. (2004).

In Paper I, we adapted the `FEWBODY` code to handle encounters involving not only single and binary stars, but also triples.[5] We use the same criteria as Fregeau et al. (2004) to decide when a given encounter is complete, defined as the point at which the separately bound hierarchies that make up the system are no longer interacting with each other or evolving internally.

To perform physical collisions between stars, `FEWBODY` uses the "sticky-star" approximation. This treats stars as rigid spheres with radii equal to their stellar radii. A physical collision is assumed to occur when the radii of the stars overlap. When this happens, the stars are merged assuming conservation of linear momentum and no mass loss. This does not account for tidal effects, which could significantly increase the collision probability (e.g. McMillan 1986), but are beyond the scope of this work. For this reason, we consider the collision probabilities presented in this paper to be lower limits for the true values.

Previous scattering experiments have shown that the total energy and angular momentum are critical parameters in deciding the outcomes of 1+2 interactions (e.g. Valtonen & Karttunen 2006). We confirmed this for higher-N interactions (up to $N = 6$) in Paper I. Therefore, we will fix the total energy and angular momentum when comparing between encounters involving different numbers of objects. By fixing these quantities, we aim to remove the dependences of the encounter outcomes on energy and angular momentum (when comparing between encounters involving different numbers of particles, or different combinations of particle types/radii), thereby normalizing the comparisons to reveal the dependences of the collision probability on other parameters, in particular the particle radii. We

[2] For a given N, there are $N+1$ total encounter scenarios, as is evident upon looking at Figure 1. For the 2+3 case, this figure illustrates that there are six interaction scenarios in total (since five particles are involved in the interaction). The coefficients for the two cases involving all identical particles are obtained directly from numerical scattering experiments. Collision probabilities are then calculated for the four remaining interaction scenarios, with different numbers of stars of types 1 and 2, using these two coefficients.

[3] In principle, the 1+2 case can even be used, but here the normalization in total energy and angular momentum is slightly more complicated (see Leigh & Geller 2012 for more details), since there is only one binary orbit going into the interaction.

[4] for the source code, see http://fewbody.sourceforge.net

[5] Specifically we created additional subroutines to simulate 1+3 and 3+3 encounters; codes to simulate encounters between binaries and singles only, as well as a 2+3 encounter code, were previously available in the `FEWBODY` package. The authors are happy to provide these additional subroutines to users of `FEWBODY` upon request.

consider one specific combination of the total energy and angular momentum (see below), for which both the total energy (range) and angular momentum are always chosen to be the same to within a factor of ~ 2 for every type of encounter (see Paper I for more details).

To this end, all orbits are circular, and have semi-major axes of either $a_0 = 0.1$ AU or $a_1 = 1$ AU. Hence, for a 2+3 encounter for example, we adopt $a_0 = 0.1$ AU for the orbital separation of the inner orbit of the triple, and $a_1 = 1$ AU for both the outer orbit of the triple and the interloping binary. For a 1+3 encounter, we similarly adopt $a_0 = 0.1$ AU and $a_1 = 1$ AU for the inner and outer orbits, respectively, of the triple, while for a 2+2 encounter we adopt $a_0 = 0.1$ AU and $a_1 = 1$ AU for the two binaries. These initial semi-major axes are summarized in Table 1. A semi-colon is used to separate different objects, whereas a comma is used to separate the orbits within triples. Parantheses are used to enclose the semi-major axes of triples, with the smaller of the two semi-major axes always corresponding to the inner binary. Note that we have checked that our results are approximately insensitive to our choice of semi-major axes, for orbital separation ratios $a_0/a_1 \lesssim 100$. For a given relative velocity at infinity and impact parameter, the choice of semi-major axes sets the encounter energy and angular momentum. Thus, while the exact collision probability does depend on the choice of semi-major axes, our method does not. This choice of semi-major axes, along with our chosen impact parameter ($b = 0$; see below), serves to minimize the computational expense of our scattering experiments, by minimizing the total angular momentum. Regardless, these semi-major axes are relatively characteristic of the multiple star systems we expect to be present in globular clusters. At least in the cluster core, only relatively compact multiples should survive for several Gyr in such dense stellar environments. This is especially true for triples (and higher-order multiples), given that they are only stable against dissociation if the ratio between their inner and outer orbital separations is sufficiently small (e.g. Mardling 2001).

For each Run, we populate a grid of scattering experiments varying only the relative velocity at infinity $v_{\rm inf}$. Specifically, we select values for the relative velocity at infinity from 0 to 1.1 in equally-spaced intervals of 0.004, in units of the critical velocity $v_{\rm crit}$ (defined as the relative velocity that gives a total energy of zero for the encounter). Hence, our chosen range of relative velocities at infinity includes the case of zero total energy. In the case $v_{\rm inf} > v_{\rm crit}$, the encounter is prompt and at least one particle is almost immediately lost from the system. For $v_{\rm inf} < v_{\rm crit}$, all particles may be temporarily bound and participate in a prolonged resonant encounter. We fix the impact parameter at $b = 0$, independent of $v_{\rm inf}$. For our assumed circular orbits, this minimizes the total angular momentum (and hence reduces the total computational cost of our simulations) while preserving our normalization that the total energy and angular momentum must be roughly the same independent of the number of interacting particles. Finally, at each point in this grid, we perform multiple scattering experiments randomizing all angles in the encounter, including the angles at impact between the orbital planes of any binaries and triples involved in the encounters. In total, we perform 24750 simulations for every Run (with the exception of Figure 4, for which we are limited to using only 4500 simulations per data point). We chose this number of simulations to balance between statistical significance and computational expense (i.e. simulation run-time). Of course, running more simulations would reduce the uncertainties on the calculated collision probabilities and yield more precise results, which may be desirable for certain applications.

The collision probability is calculated from the output of our numerical scattering experiments for a given encounter type and a given Run as:

$$P_{\rm coll} = \frac{N_{\rm coll}}{N_{\rm tot}}, \tag{6}$$

where $N_{\rm coll}$ is the total number of encounters that result in a direct physical collision, and $N_{\rm tot}$ is the total number of encounters performed (throughout this paper, $N_{\rm tot} = 24750$, except for Figure 4, as stated above). The uncertainty for the collision probability is calculated using Poisson statistics according to:

$$\Delta P_{\rm coll} = \left(\left(\frac{\sqrt{N_{\rm coll}}}{N_{\rm tot}} \right)^2 + \Delta P_{\rm coll,int}^2 \right)^{1/2}, \tag{7}$$

where $\Delta P_{\rm coll,int}$ is an additional term to account for any intrinsic dispersion in our calculated collision probabilities (see Section 3 for our assumed values of $\Delta P_{\rm coll,int}$). This additional source of dispersion comes from a combination of numerical inaccuracies, our normalization in energy and angular momentum, and subtle inadequacies of our model in capturing all of the relevant underlying physics (e.g. the issue of saturation which we discuss in more detail in Section 3).[6] Technically, this uncertainty should include scattering experiments that result in unresolved outcomes (Hut 1983b). However, we find that the number of unresolved outcomes is sufficiently small that it does not significantly contribute to $\Delta P_{\rm coll}$, and we do not include it in its calculation.

3 RESULTS

In this section, we first present some example applications of our method. Using these, we go on to describe how to calculate collision probabilities for any number of particles and any combination of particle radii, as well as for a limited range of particle masses.

3.1 Different particle radii

First, consider the case where the particles all have the same mass, but two different particle radii are possible. We assume $R_1 = 0.1$ R$_\odot$ and $R_2 = 5$ R$_\odot$, and $m_1 = m_2 = 1$ M$_\odot$. Figure 1 shows the results of a series of numerical scattering simulations of binary-triple encounters (i.e. $N = 5$). Here, we vary the number of large particles from 0 to 5, as shown on the x-axis. The constants σ_{11} and σ_{22} in Equation 4 are calculated from our numerical scattering experiments using the $N_1 = 5$ and $N_2 = 5$ cases, where all particles are either

[6] Formally, the intrinsic dispersion term $\Delta P_{\rm coll,int}$ should be found by forcing the reduced chi-square of a fit to be unity. However, in our case, we have only three data points (i.e. $N = 4$, 5 and 6) to work with in calculating the intrinsic dispersion term. Thus, necessarily, our estimates for $\Delta P_{\rm coll,int}$ are only approximate.

Table 1. Initial semi-major axes of all binaries and triples

Encounter Type	Semi-major axes (in AU)
2+2	0.1; 1.0
1+3	(0.1, 1.0)
2+3	1.0; (0.1, 1.0)
3+3	(0.1, 1.0); (0.1, 1.0)

of type 1 (α_{11}) or type 2 (α_{22}). The constant α_{12} is then calculated from Equation 5. The open points show the results of these calculations, and are compared directly to our numerical scattering experiments via the filled points. Error bars are calculated using Equation 7 with $\Delta P_{\rm coll,int} = 0.05$, which is chosen to ensure that the residuals calculated in Figure 1 are all within one standard deviation of zero. Our calculated predictions agree very well with the results of our numerical scattering experiments, and are within one standard deviation of each other in all cases. The agreement is slightly worse for the $N_2 = 1$ and $N_2 = 2$ cases, however, for which our calculated collision probabilities deviate from our numerical scattering experiments by about one standard deviation (see the bottom panel in Figure 1). The reason for this poor agreement is not understood. This may be highlighting that we are missing some higher-order term(s) in Equation 4, possibly related to our calculation of the coefficient σ_{12}. Regardless, the calculated collision probabilities (via Equation 4) always agree with the results of our numerical scattering experiments to within a couple percent or better.

In Figure 2 we show the results of a series of 2+2 (filled circles), 1+3 (open circles), 2+3 (filled triangles) and 3+3 (open stars) encounters, this time involving all identical particles. The encounter parameters are the same as in Figure 1 and Table 1, with the sole exception that the particle radii are all identical. For each encounter type, we show the collision probability as a function of the ratio R/a_0, where R is the particle radius and a_0 is the initial semi-major axis of the most compact orbit going into the encounter (i.e. $a_0 =$ 0.1 AU). Hence, $R/a_0 = 1$ corresponds to a contact configuration for the most compact orbit initially.

The key point is that an analogous version of Figure 1 can be made for any combination of particle radii (i.e. any R_1 and R_2). In principle, this can be done by extracting the coefficients σ_{11} and σ_{22} directly from Figure 2, and fitting a curve to these data to derive the collision probability at any value of R (and N). The temptation is, for every N, to fit the data with a function of the form:

$$P_{\rm coll} = \delta R^{\gamma} \binom{N}{2} \tag{8}$$

However, as is clear from Figure 2, a plot of R versus $P_{\rm coll}$ is clearly sub-linear. Even in log-log space, significant curvature is apparent. This is not unexpected, since in the limits $R \rightarrow 0$ and $R \rightarrow a_0$ (where a_0 is the semi-major axis of the most compact orbit going into the encounter) we expect, respectively, $P_{\rm coll} \rightarrow 0$ and $P_{\rm coll} \rightarrow 1$, independent of the number of interacting particles N. Thus, the coefficients δ and γ in Equation 8 are not constants, but are instead functions of the particle radius R. (In practice, one could fit a function similar to Equation 8 to a subset of data around the desired value of R/a_0, in order to derive the collision probability at a point not plotted in Figure 2).

Since here, by construction, the total encounter energy and angular momentum are roughly the same independent of N, then, via the binomial theorem, at a given value of the particle radius R, δ and γ should be the same for all N. That is, since the particles are all identical and the total encounter energy and angular momentum are fixed, the collision probability should vary only with the number of interacting particles N. To illustrate this point, we calculate the quantity $P_{\rm coll}/\binom{N}{2} = \alpha_{\rm ii}$ for encounters involving all identical particles, for all values for the particles radius, R, shown in Figure 2, with the expectation that the ratio $P_{\rm coll}/\binom{N}{2}$ will be the same for all N (to within the uncertainties). The results are shown in Table 2 and Figure 3. Uncertainties are calculated using Equation 7 with $\Delta P_{\rm coll,int} = 0.01$, which ensures that our simulated collision probabilities for the 2+2 and 1+3 cases are always within one standard deviation of each other.

The quantity $P_{\rm coll}/\binom{N}{2}$ is approximately the same (e.g., within typically less than one standard deviation) for all N at a given particle radius R, until reaching a "saturation" limit at $\log(R/a_0) \gtrsim -1.5$. This suggests that, at least for a given particle radius R, the collision probabilities for 2+3 and 3+3 encounters can be calculated directly from the collision probability for the 2+2 (or 1+3) case, without having to run any 2+3 and 3+3 numerical scattering experiments. This offers the potential to calculate collision probabilities for high-N interactions with minimal computational expense, which increases steeply with increasing N (as we also point out in Paper I). Equivalently, for fixed computational expense a larger number of simulations can be performed for lower N interactions, which subsequently increases the statistical significance and accuracy of the results. We caution that the simulated data begin to deviate from the trend that $P_{\rm coll}/\binom{N}{2}$ is roughly independent of N near the saturation limit $P_{\rm coll} \rightarrow 1$. As shown in Figure 3, this begins around $\log(R/a_0) \sim -1.5$, and should be treated with caution. More work is needed to verify that this exact saturation limit is ubiquitous for all total encounter energies and angular momenta. In general, however, adopting larger initial semi-major axes a_0 pushes the saturation limit to larger values of the particle radius R.

3.2 Different particle masses

Next, we consider encounters involving particles having different radii *and* different masses. The key point we wish to illustrate in this section is that, provided the range of energies and angular momenta are fixed and independent

Table 2. The quantity $P_{\rm coll}/\binom{N}{2}$ as a function of the particle radius R

Particle Radius (in $R_\odot$)	$P_{\rm coll}/\binom{N}{2}$ (2+2; N=4)	(1+3; N=4)	(2+3; N=5)	(3+3; N=6)
0.005	0.0042 ± 0.0017	0.0059 ± 0.0017	0.0052 ± 0.0010	0.0060 ± 0.0007
0.01	0.0069 ± 0.0017	0.0085 ± 0.0017	0.0087 ± 0.0010	0.0089 ± 0.0007
0.05	0.0203 ± 0.0017	0.0231 ± 0.0017	0.0219 ± 0.0010	0.0213 ± 0.0007
0.1	0.0304 ± 0.0017	0.0333 ± 0.0017	0.0307 ± 0.0011	0.0278 ± 0.0007
0.5	0.0618 ± 0.0018	0.0633 ± 0.0018	0.0524 ± 0.0011	0.0434 ± 0.0007
1.0	0.0773 ± 0.0018	0.0770 ± 0.0018	0.0610 ± 0.0011	0.0481 ± 0.0008
5.0	0.1255 ± 0.0019	0.1252 ± 0.0019	0.0785 ± 0.0011	0.0564 ± 0.0008
10.0	0.1581 ± 0.0020	0.1567 ± 0.0020	0.0896 ± 0.0012	0.0667 ± 0.0008
20.0	0.1667 ± 0.0020	0.1667 ± 0.0020	0.1000 ± 0.0012	0.0667 ± 0.0008

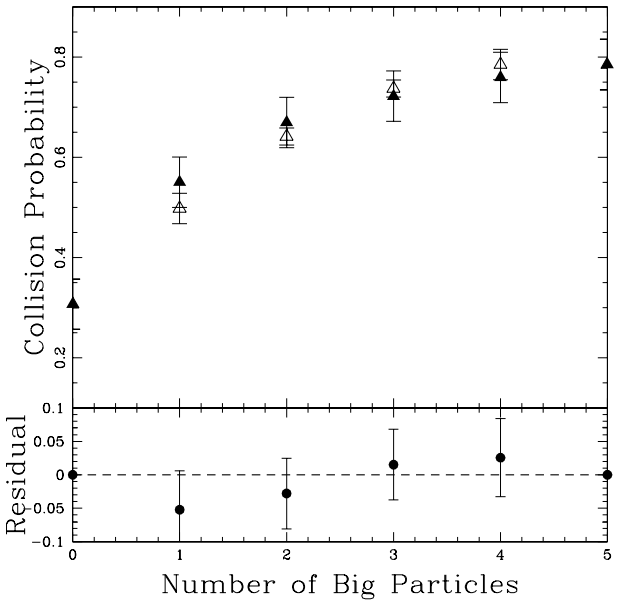

Figure 1. The probability of a collision occurring during a binary-triple encounter, shown in the top panel. Two particle radii are considered, namely $R_1 = 0.1$ $R_\odot$ and $R_2 = 5$ $R_\odot$. The number of large particles is shown on the x-axis, and the collision probability is shown on the y-axis. All particle masses are identical, and the range of total encounter energies and angular momenta over which we integrate are identical for all cases (i.e. combinations of small and large particles). We adopt $a_0 = 0.1$ AU for the orbital separation of the inner orbit of the triple, and $a_1 = 1$ AU for both the outer orbit of the triple and the interloping binary. All orbits have eccentricities of zero, initially. The open triangles show our predictions for the collision probabilities, calculated from Equations 4 and 5 using the results of our numerical scattering experiments for the $N_1 = 0$ and $N_2 = 5$ cases (i.e. all small and all large particles). The filled triangles show the same collision probabilities, but calculated directly from the results of the corresponding numerical scattering experiments. Error bars are calculated using Poission statistics (filled triangles) and simple error propagation (open triangles), beginning with Equation 7 and assuming $\Delta P_{\rm coll,int} = 0.05$. The bottom panel shows the residuals between the collision probabilities calculated directly from our numerical scattering experiments (filled triangles) and our model predictions (open triangles). The dashed line is shown for reference, and represents perfect agreement between our model and the data.

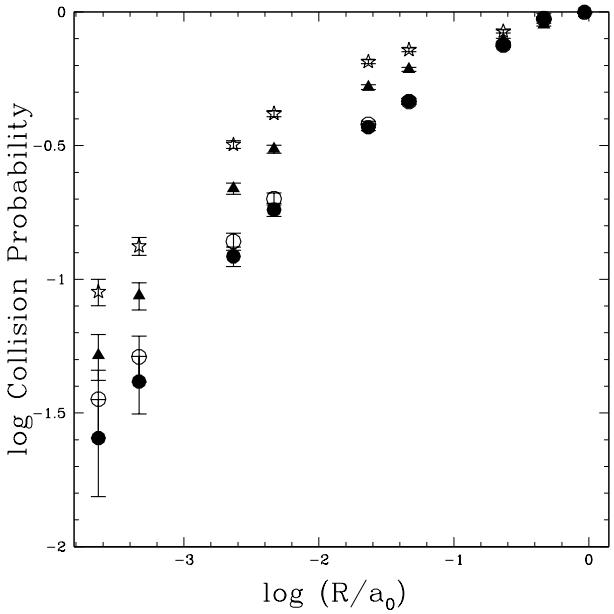

Figure 2. The logarithm of the probability of a collision occurring during encounters involving all identical particles is shown as a function of the logarithm of the ratio R/a_0, where R is the particle radius in AU and $a_0 = 0.1$ AU is the initial semi-major axis of the most compact orbit going into the encounter. Hence, we adopt $a_0 = 0.1$ AU for the orbital separations of the inner orbits of any triples, and $a_1 = 1$ AU for the outer orbits of any triples. For the 2+3 case, the initial semi-major axis of the binary is $a_1 = 1$ AU, whereas for the 2+2 case the binaries have different initial semi-major axes of $a_0 = 0.1$ AU and $a_1 = 1$ AU. Thus, a_0 is a constant for all encounters, independent of the total number of particles or the particle radii. The filled circles, open circles, filled triangles and open stars correspond to 2+2, 1+3, 2+3 and 3+3 encounters, respectively. Error bars are calculated using Equation 7 with $\Delta P_{\rm coll,int} = 0.01$.

of N, Equation 3 is approximately valid and describes the collision probabilities to within a few percent, *independent of the distribution of particle masses, provided they are all within a factor* $\lesssim 2$. Figure 4 shows two such examples. The first is shown by the open triangles, for which the particle masses are fixed and independent of our choices for the particle radii. We set the particle masses to 0.7, 0.8, 0.9, 1.0 and 1.0 $M_\odot$, with particle radii of either $R_1 = 0.1$ $R_\odot$ or

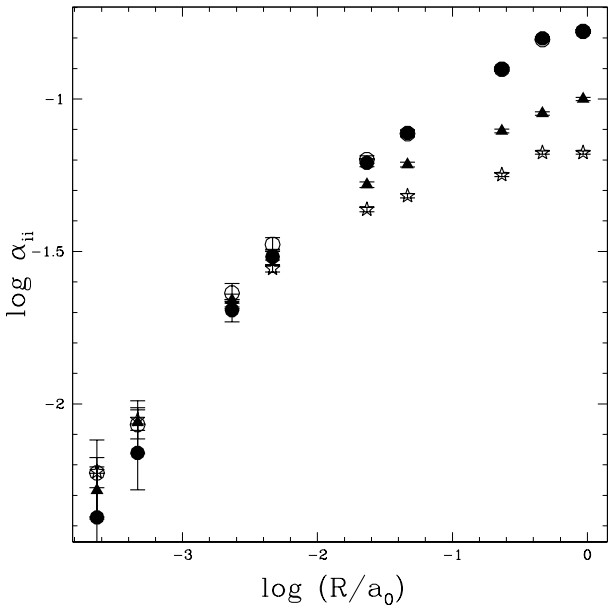

Figure 3. The logarithm of the coefficient $\alpha_{\rm ii}$ given in Table 2, calculated as $P_{\rm coll}/\binom{N}{2}$, as a function of the logarithm of the ratio R/a_0, where R is the particle radius in AU and $a_0 = 0.1$ AU is the initial semi-major axis of the most compact orbit going into the encounter, for encounters involving all identical particles. We assume the same encounter parameters and symbols as in Figure 2. Error bars are calculated as in Figures 1 and 2.

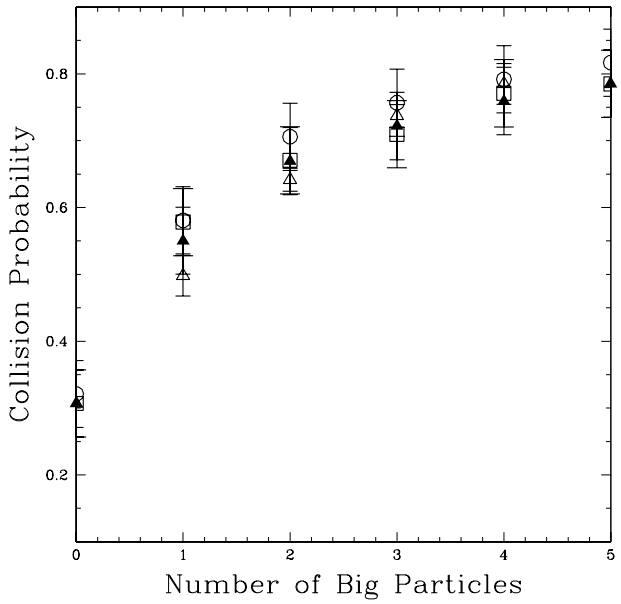

Figure 4. The probability of a collision occurring during a binary-triple encounter. We assume the same encounter parameters and particle radii as in Figure 1. This time, however, the particle masses can be different. The open and filled triangles show the same collision probabilities as in Figure 1, and assume all equal mass particles (i.e. 1 $M_\odot$). That is, the open triangles are calculated from Equations 4 and 5 using the results of our numerical scattering experiments for the $N_1 = 0$ and $N_2 = 5$ cases only, and the filled triangles show the same collision probabilities but calculated directly from the results of the corresponding numerical scattering experiments. The open circles show the same encounter parameters as in Figure 1 and are calculated directly from our numerical scattering experiments, but assuming particle masses of 0.7, 0.8, 0.9, 1.0 and 1.0 $M_\odot$ for every simulation. The open squares again show the same encounter parameters and are calculated directly from our numerical scattering experiments, but adopting radii and masses of $R_1 = 0.1$ $R_\odot$ and $m_1 = 0.5$ $M_\odot$ for particles of type 1, while particles of type 2 have radii $R_2 = 5$ $R_\odot$ and masses $m_2 = 1$ $M_\odot$. Error bars are calculated as in Figure 1 (i.e. using Equation 7 with $\Delta P_{\rm coll,int} = 0.05$).

$R_2 = 5$ $R_\odot$ assigned randomly (i.e. independent of particle mass). The initial configuration (i.e. which objects form the inner binary of the triple, etc.) is also chosen at random. The second example is shown by the open squares. Here, we vary the particle masses along with the particle radii, such that particles of type 1 have $R_1 = 0.1$ $R_\odot$ and $m_1 = 0.5$ $M_\odot$, while particles of type 2 have $R_2 = 5$ $R_\odot$ and $m_2 = 1$ $M_\odot$. Again, the initial configuration is then chosen at random. Figure 4 shows that in both of these examples, Equation 3 accurately describes the collision probabilities to within a few percent. We have checked that this is also the case for mass ratios ~ 0.05, however a more thorough exploration of the relevant parameter space is required to accurately determine to what mass ratios this approximation holds. Our results support the conclusion that it is valid for mass ratios $\gtrsim 0.5$, and possibly much lower.

3.3 Putting it all together

In this section, we combine the results of the previous two sections to construct a simple procedure for calculating collision probabilities in realistic star clusters, for any combination of particle radii and masses. Thus far, we have focussed on encounters involving only two different types of particles. The method presented below, however, is more general.

To summarize, our method is as follows:

- Decide upon the encounter type and, in particular, the total number of particles involved in the interaction. As a guide, the observed fractions of binary and multiple star systems can be used to calculate analytic estimates for the rates of the different encounter types (e.g. 2+2, 2+3, etc., see Leonard 1989; Leigh & Sills 2011).
- Determine the initial total encounter energy and angular momentum from the initial orbital eccentricities and semi-major axes, along with the initial relative velocity at infinity and impact parameter. Note that the method is valid both for a particular combination of energy and angular momentum, as well as consistent ranges in these quantities. Depending on how much information is available, one might estimate the relative velocities at infinity and the impact parameter in a star cluster from the observed surface brightness and velocity dispersion profiles (e.g. Leonard 1989; Bahramian et al. 2013). Likewise, binary orbital parameters and masses can be drawn from the appropriate observed (or assumed) distribution functions.
- Set the particle types, in particular the particle radii $R_{\rm i}$, along with the particle masses. Note that, as shown in Section 3.2, our method is valid to within a few percent for

any combination of particle masses (to within a factor of a few).[7]

• Given the particle radii, obtain the coefficients $\alpha_{\rm ii}$, $\alpha_{\rm jj}$, etc. directly from numerical scattering experiments, using the parameters determined above. With these, calculate the coefficient(s) $\alpha_{\rm ij}$ using the generalized equation:

$$\alpha_{\rm ij} = \frac{\alpha_{\rm ii}\sigma_{\rm ii} + \alpha_{\rm jj}\sigma_{\rm jj}}{\sigma_{\rm ii} + \sigma_{\rm jj}}, \quad (9)$$

where $\sigma_{\rm ii} = 2\pi R_{\rm i}^2$. As shown in Figure 2, nearly all possible values of the coefficients $\alpha_{\rm ii}$, $\alpha_{\rm jj}$, etc. can be covered using a limited number of numerical scattering experiments by extrapolating between data points. Additionally, numerical scattering experiments need only be run for the 2+2 or 1+3 cases since, using the binomial theorem, the corresponding coefficients for higher-N interactions (2+3, 3+3, etc.) can be calculated directly (e.g., see end of Section 3.1). This significantly reduces the total computational expense for higher-N interactions, since the integration times for the simulations increase dramatically with increasing particle number.

• Calculate the desired collision probabilities using the generalized formula:

$$P_{\rm coll} = \sum_{\rm i=1}^{\rm N_i} \alpha_{\rm ii} \binom{N_{\rm i}}{2} + \frac{1}{2} \sum_{\rm i=1}^{\rm N_i} \sum_{\rm j=1, i\neq j}^{\rm N_j} \alpha_{\rm ij} \binom{N_{\rm i}}{1} \binom{N_{\rm j}}{1} \quad (10)$$

As a proof of concept of the above generalized methodolgy, consider 2+3 encounters involving three different particle types characterized by their different radii, or $R_1 = 0.05$ R$_\odot$, $R_2 = 0.5$ R$_\odot$ and $R_3 = 5.0$ R$_\odot$. All particles have the same mass of 1 M$_\odot$, and the semi-major axes and eccentricities are chosen to be the same as used in Figure 2 and Table 2, as is the range of relative velocities at infinity (including a small fraction of encounters with positive total energies). As before, the impact parameter is set equal to zero for all simulations. We consider five different combinations of particle types, and run 24750 simulations for each such combination. For comparison, we calculate the corresponding collision probabilities (along with their uncertainties $\sigma P_{\rm coll}$) using Equations 10 and 9 as well as the coefficients $\alpha_{\rm ii}$ and $\alpha_{\rm jj}$ obtained from Table 2. Based on Figure 3, $R_3 = 5$ R$_\odot$ is beyond the saturation limit for our model. This will introduce some small amount of additional scatter into our calculations for the collision probabilities. To account for this additional source of uncertainty, we calculated the mean value of $\alpha_{\rm ii}$ at $R = 5$ R$_\odot$ in Figure 3 for all values of the particle number N (i.e. $N = 4$, 5 and 6), and added the resulting value to its uncertainty (in quadrature) using Equation 7 with $\Delta P_{\rm coll,int} = 0.03$. This serves to illustrate the importance of accurately estimating the coefficients $\alpha_{\rm ii}$, $\alpha_{\rm jj}$, etc. when calculating collision probabilities.

The results of this example are shown in Table 3. The agreement between our simulated and calculated collision probabilities is quite good in all cases, which generally agree to within a few percent.

[7] In a real star cluster, the distribution of stellar masses and radii is continuous. Hence, some binning by stellar mass (which is tightly correlated with stellar radius on the main-sequence) is desirable, wherever this assumption is reasonable. For example, binning is a reasonable assumption for interactions involving white dwarfs, bright red giants and/or main-sequence stars close to the turn-off. Here, the objects all have very similar radii and masses *within* their individual stellar evolution-based classifications, but very different radii *between* these classifications.

4 SUMMARY AND DISCUSSION

In this paper, we present a formalism for calculating collision probabilities during chaotic gravitational encounters with finite-sized particles. The interactions involve any number of particles and any combination of particle radii, using a minimal number of numerical scattering experiments. Our method relies on the binomial theorem, and can also be extended to encounters involving particles of different masses (see below).

Our model is applicable for a constant value or range in the total encounter energy and angular momentum. Hence, our formalism for the collision probability can be extended to include any combination of total encounter energy and angular momentum. To do this, plots analogous to Figure 2 are generated for different total encounter energies at fixed angular momentum (and vice versa). From here, the dependence of the fitting parameters (see Equation 8) on the total encounter energy and angular momentum is derived. In general, the collision probability decreases with increasing total encounter energy (i.e. becomes less negative and thus closer to zero), and with increasing total angular momentum. Depending on the difficulties associated with any curvature in log-log space (which prohibits fitting a constant power-law to the data), an analytic formula for the collision probability can be derived by running additional numerical scattering experiments to cover the full range in encounter energies and angular momenta. The resultant formula would thus cover the entire range of the relevant parameter space (total encounter energy and angular momentum, distribution of particle masses and radii, particle number, etc., in, for example, open, globular or nuclear star cluster clusters). Alternatively, our method can be used to create a library of collision probabilities, again covering the entire range of the relevant parameter space while minimizing the total number of numerical scattering experiments that need to be performed (by extrapolating between data points, as in Figure 2). This will be the focus of future work.

Our formalism is valid as well for different particle masses, provided they are all within a factor of $\sim$ a few. This is because changing the particle masses also changes the total encounter energy and angular momentum. Thus, by fixing the total energy and angular momentum for all encounters, the dependence of the collision probability is removed, at least to first-order. There are second-order effects related to the lifetime of the system, causing slightly higher collision probabilities for encounters with large particle mass ratios. However, the deviation is by at most a few percent from the model presented in this paper, which assumes all equal mass particles.

Our method is ideal for application in old open and globular clusters, since it is applicable over a wide range of particle radii but a relatively narrow range of particle masses. Suitable interactions occur in GCs when single, binary and triple stars undergo encounters, since the objects involved include main-sequence stars (close to the turn-off), red or asymptotic giant branch stars, white dwarfs and neu-

Table 3. The collision probability during 2+3 encounters for various combinations of particle types 1, 2 and 3

Number of Each Type of Particle			Collision Probability	
N_1 $R_1 = 0.05$ R$_\odot$	N_2 $R_2 = 0.5$ R$_\odot$	N_3 $R_3 = 5.0$ R$_\odot$	Simulated $P_{\rm coll} \pm \sigma P_{\rm coll}$	Calculated $P_{\rm coll} \pm \sigma P_{\rm coll}$
4	1	0	0.3324 ± 0.0042	0.3398 ± 0.0074
4	0	1	0.5264 ± 0.0057	0.4454 ± 0.1397
3	2	0	0.4084 ± 0.0048	0.4307 ± 0.0073
3	1	1	0.5670 ± 0.0060	0.5357 ± 0.1103
1	1	3	0.7221 ± 0.0071	0.7578 ± 0.1807

tron stars. All of these objects have masses that are typically the same to within a factor $\lesssim 2$, but radii differing by several orders of magnitude. Thus, the geometric cross-section dominates the total collisional cross-section for these objects, as opposed to the gravitationally-focused cross-section. For example, consider an average encounter in a typical GC, involving mostly white dwarfs. If even a single main-sequence star is included in the interaction, then the collision probability can increase by nearly an order of magnitude (this is the case for, e.g. the encounter parameters assumed in Figure 2, for which the collision probability begins to saturate at the particle radius corresponding to that of a typical main-sequence star in an old globular cluster).[8] Consider a 2+2 interaction with the same encounter parameters as adopted in Figure 2 and Table 2. If the interaction involves only white dwarfs, then $\rm P_{coll} \sim 0.04$. If one of the white dwarfs is replaced by a single (near turn-off) main-sequence star, then $\rm P_{coll} \sim 0.25$. Conversely, consider the same encounter but involving only main-sequence stars with masses close to the turn-off mass. The collision probability for this encounter is $\rm P_{coll} \sim 0.46$, roughly an order of magnitude larger than calculated for the same encounter but involving only white dwarfs. Here, if a single main-sequence star is replaced by a white dwarf, then the collision probability changes to $\rm P_{coll} \sim 0.31$.

ACKNOWLEDGMENTS

We would like to thank Christian Knigge for useful discussions and suggestions. N. W. C. L. is grateful for the generous support of an NSERC Postdoctoral Fellowship. A. M. G. is funded by a National Science Foundation Astronomy and Astrophysics Postdoctoral Fellowship under Award No. AST-1302765.

REFERENCES

Bahramian A., Heinke C. O., Sivakoff G. R., Gladstone J. C. 2013, ApJ, 766, 136
Binney J., Tremaine S., 1987, Galactic Dynamics (Princeton: Princeton University Press)
Brockamp M., Baumgardt H., Kroupa P. 2011, MNRAS, 418, 1308
Brown W. R., Geller M. J., Kenyon S. J., Kurtz M. J. 2005, ApJL, 622, L33
Brown W.R., Cohen J. G., Geller M. J., Kenyon S. J. 2012, ApJL, 754, L2
Cohn H., Kulsrud R. M. 1978, ApJ, 226, 1087
Demarque P., Virani S. 2007, A&A, 461, 651
Fregeau J. M., Cheung P., Portegies Zwart S. F., Rasio F. A. 2004, MNRAS, 352, 1
Fregeau J. M., Ivanova N., Rasio F. A. 2009, ApJ, 707, 1533
Geller A. M., Mathieu R. D., Harris H. C., McClure R. D. 2008, AJ, 135, 2264
Geller A. M., Hurley J. R., Mathieu R. D. 2013, AJ, 145, 8
Goldreich P., Lithwick Y., Sari R. 2004, ARA&A, 42, 549
Heggie D. C., Hut P. 2003, The Gravitational Million-Body Problem: A Multidisciplinary Approach to Star Cluster Dynamics (Cambridge: Cambridge University Press) Tout C. A. 2000, MNRAS, 315, 543
Henon M. 1969, A&A, 1, 223
Hurley J. R., Pols O. R., Aarseth S. J., Tout C. A. 2005, MNRAS, 363, 293
Hut P. 1983, ApJL, 272, L29
Hut P. 1983, ApJ, 268, 342
Hut P., Verbunt F. 1983, Nature, 301, 587
Hut P., Murphy B. W., Verbunt F. 1991, A&A, 241, 137
Hut P., McMillan S., Romani R. W. 1992, ApJ, 389, 527
Leigh N., Knigge C., Sills A. 2007, ApJ, 661, 210
Leigh N., Sills A. 2011, MNRAS, 410, 2370
Leigh N., Geller A. M. 2012, MNRAS, 425, 2369
Leigh N., Geller A. M. 2013, MNRAS, 432, 2474
Leigh N., Giersz M., Webb J. J., Hypki A., De Marchi G., Kroupa P., Sills A. 2013, MNRAS, 436, 3399
Leonard P. J. T. 1989, AJ, 98, 217
Liouville J. 1838, Journ. de Math., 3, 349
Lithwick Y., Chiang E. 2007, ApJ, 656, 524
Maeder A. 2009, Physics, Formation and Evolution of Rotating Stars. Berlin: Springer-Verlag
Mapelli M., Zampieri L. 2014, ApJ, 794, 7
Mardling R. A., 2001, in Podsiadlowski P., Rappaport S., King A. R., D'Antona F., Burderi L., eds, ASP Conf. Ser. Vol. 229, Evolution of Binary and Multiple Star Systems. Astron. Soc. Pac., San Francisco, p. 101
McMillan S. L. W., 1986, ApJ, 306, 552
Merritt D. 2013, Dynamics and Evolution of Galactic Nuclei (Princeton: Princeton University Press)
Miller M., Davies M. B. 2012, ApJ, 755, 81

[8] The coefficients α_{11} and α_{22} for main-sequence stars and white dwarfs, respectively, are obtained from Table 2, and the coefficient α_{12} is then calculated using Equation 5. The collision probability is subsequently calculated using Equation 4.

Monaghan J. J. 1976, MNRAS, 176, 63
Monaghan J. J. 1976, MNRAS, 177, 583
Naoz S., Fabrycky D. C. 2014, ApJ, 793, 137
Newton, I. 1760, Philosophiae Naturalis Principia Mathematica (Trinity College: Regalis Societatis Praesses)
Perets H. B., Fabrycky D. C. 2009, ApJ, 697, 1048
Poincare H. 1892, Les methodes nouvelles de la mechanique celeste (Paris: Gauthier-Villars)
Roberts I. D., Parker L. C., Joshi G. D., Evans F. A. 2014, MNRAS, accepted (arXiv:1411.7274)
Sesana A., Sartore N., Devecchi B., Possenti A. 2012, MNRAS, 427, 502
Sigurdsson S., Phinney E. S. 1993, ApJ, 415, 631
Sigurdsson S., Phinney E. S. 1995, ApJS, 99, 609
Sills A., Bailyn C. D. 1999, ApJ, 513, 428
Spitzer L. Jr. 1987, Dynamical Evolution of Globular Clusters (Princeton, NJ: Princeton Univ. Press)
Stone N., Loeb A. 2012, MNRAS, 422, 1933
Valtonen M., Karttunen H. 2006, The Three-Body Problem (Cambridge: Cambridge University Press)
Verbunt F. 1987, ApJL, 312, L23
Verbunt F., Lewin W. H. G., van Paradijs J. 1989, MNRAS, 241, 51
Vesperini E., Heggie D. C. 1997, MNRAS, 289, 898

This paper has been typeset from a TEX/ LATEX file prepared by the author.